10-2018

X-ray *Swift* Observations of SN 2018cow

L E. Rivera Sandoval

T J. Maccarone

A Corsi

P J. Brown

David Pooley
Trinity University, dpooley@trinity.edu

See next page for additional authors

Authors

L E. Rivera Sandoval, T J. Maccarone, A Corsi, P J. Brown, David Pooley, and J C. Wheeler

X-ray *Swift* observations of SN 2018cow

L.E. Rivera Sandoval[1]⋆, T.J. Maccarone[1], A. Corsi[1], P.J. Brown[2], D. Pooley[3],
J.C. Wheeler[4]

[1]*Department of Physics and Astronomy, Box 41051, Science Building, Texas Tech University, Lubbock, TX 79409-1051, USA*
[2]*George P. and Cynthia Woods Mitchell Institute for Fundamental Physics & Astronomy, Texas A. & M.*
University, Department of Physics and Astronomy, 4242 TAMU, College Station, TX 77843, USA
[3]*Department of Physics and Astronomy, Trinity University, San Antonio, TX, USA ; Eureka Scientific, Inc., USA*
[4]*Department of Astronomy, University of Texas at Austin, Austin, TX, USA*

18 July 2018

ABSTRACT
Supernova (SN) 2018cow is an optical transient detected in the galaxy CGCG 137–068. It has been classified as a SN due to various characteristics in its optical spectra. The transient is also a bright X-ray source. We present results of the analysis of ~ 62 ks of X-ray observations taken with the *Neil Gehrels Swift Observatory* over 27 days. We found a variable behavior in the $0.3 - 10$ keV X-ray light curve of SN 2018cow, with variability timescales of days. The observed X-ray variability could be due to the interaction between the SN ejecta and a non-uniform circum-stellar medium, perhaps related to previous mass ejections from a luminous-blue-variable-like progenitor.

Key words: supernovae: individual: SN 2018cow – X-rays: stars – gamma-ray burst: general

1 INTRODUCTION

SN 2018cow (also known as ATLAS18qqn) is an optical transient detected on 16 June 2018 (10:35:02 UT) with the Asteroid Terrestrial-impact Last Alert System (ATLAS) located at Haleakala and Mauna Loa, Hawaii, USA (Smartt et al. 2018).

The position of the transient (RA=$16^h16^m00^s.22$, Dec=+$22°16'04".8$; J2000) is coincident with that of the galaxy CGCG 137–068, which is located at a redshift of 0.014[1], corresponding to a luminosity distance of 59.7 ± 4.2 Mpc (assuming $H_0 = 73.0 \pm 5$ km sec^{-1} Mpc^{-1}). SN 2018cow was initially thought to be a cataclysmic variable (CV) star (Smartt et al. 2018). However, spectral observations taken on 18 June 2018 UT found a featureless spectrum (Perley 2018). Observations taken on 19 June 2018 UT revealed the presence of Ca II H&K absorption features at the redshift of CGCG 137–068, thus confirming that SN 2018cow was in fact an extragalactic transient (Jones et al. 2018). The first X-ray observations of SN 2018cow taken with the *Neil Gehrels Swift Observatory* also on 19 June 2018 (starting at 10:34:53 UT; Rivera Sandoval & Maccarone 2018a,b) showed that the object had a 0.3-10 keV

flux of $(2.6 \pm 0.3) \times 10^{-11}$ erg cm^{-2} s^{-1}, and a hard spectrum with a photon index of $\Gamma = 1.6 \pm 0.1$. These observations also helped to discard the hypothesis that SN 2018cow was a CV, since at a distance limit of ~ 700 pc derived from its optical luminosity[2] (V=13.8 mags, Rivera Sandoval & Maccarone 2018a), the object would have an X-ray luminosity $L_X \sim 1.5 \times 10^{33}$ erg s^{-1}, which is much higher than those of typical CVs in outburst ($L_X \lesssim 10^{32}$ erg s^{-1}, see e.g. Ramsay et al. 2001; Saitou et al. 2012). Instead, these X-ray observations suggested that the object could be a Gamma-Ray Burst (GRB) afterglow. GRB afterglows have X-ray luminosities in the range $10^{43} - 10^{46}$ erg s^{-1} at ~ 24 hrs after trigger (D'Avanzo et al. 2012), and SN 2018cow at the distance of ~ 60 Mpc would have an X-ray luminosity $L_X \sim 1.15 \times 10^{43}$ erg s^{-1}. X-ray luminosities of Type Ib/Ic supernovae after few days of the explosion are below 10^{42} erg s^{-1} (Drout et al. 2016), slightly lower than the observed luminosity of the transient. Alternatively, the X-rays could merely represent a rather extreme shock breakout.

No γ-rays in the 14–195 keV range were detected with *Swift*/BAT around the time of optical discovery (Lien et al. 2018). *Fermi*/GBM did not detect activity spatially coincident with SN 2018cow (Dal Canton et al. 2018) in the period

---

⋆ E-mail: liliana.rivera@ttu.edu
[1] Value obtained from the NASA/IPAC extragalactic database http://ned.ipac.caltech.edu/forms/byname.html.

[2] Assuming a typical absolute optical magnitude for CVs in outburst $M_V \sim 4.5$ (Warner 1987).

13-16 June 2018, but it is possible that the event occurred outside the field of view of such telescope because the sky region of the transient was observed only 54% of the time during that period (this could be the case for *Swift*/BAT as well). Additionally, no detection at TeV energies were made in the period 13-16 June 2018 UT with *HAWC* in the direction of the transient (Garcia-Gonzalez et al. 2018). Ultraviolet observations carried out on 19 June 2018 (10:40:40 UT) with the UVOT instrument on board of *Swift*, showed that SN 2018cow was also bright at such wavelengths, with Vega magnitude of 11.70 ± 0.01 (Rivera Sandoval & Maccarone 2018a).

SN 2018cow was also identified at millimetre wavelengths with NOEMA on 20 June 2018 UT, with a flux of ~ 6 mJy at 90 GHz (de Ugarte Postigo et al. 2018). On 22 June 2018 UT the object had a flux density of ~ 0.5 mJy determined using data from AMI-LA at a central frequency of 15.5 GHz (Bright et al. 2018). ATCA detected the transient at 34 GHz with a flux of ~ 5.6 mJy on 26 June 2018 UT (Dobie et al. 2018a). The flux in that band increased to ~ 7.6 mJy two days later (Dobie et al. 2018b).

From spectroscopic observations of SN 2018cow carried out on 20 June 2018 UT with the Xinglong-2.16m, Xu et al. (2018) reported a broad bump or absorption feature (He I [3889] if absorption) and a broad feature at 5040 Å that could be the signature of high velocity blending as in broadline Type Ic supernovae (SNe BL-Ic). Izzo et al. (2018) reported further spectroscopic follow up with ISIRIS/GTC on 21 June finding broad undulations similar to SNe BL-Ic, though without a direct match, though absorption blueward of a 5460 Å peak could be FeII at 20,000 km s^{-1}. Srivastav et al. (2018) reported on the evolution of the 4500/5500 Å feature, finding it to have strengthened until 5 days after discovery and then weaking to almost disappear in Liverpool Telescope spectra taken on 24 June. This would be unusual for a SN emerging from a fading afterglow and/or shock breakout. From spectra taken on 8 July UT, 22 days after discovery, Benetti et al. (2018) identified emission features that could be associated to He lines, thus re-classifying SN 2018cow as a Type Ib SN.

In this letter we present results of the analysis of 27 days of continuous X-ray follow-up observations of SN 2018cow with *Swift* in the 0.3–10keV energy band, starting approximately three days after its discovery.

2   OBSERVATIONS

The ~ 62 ks of X-ray *Swift* observations analyzed in this letter cover the period from 19 June 2018 to 13 July 2018 UT. These are a total of 72 observations with exposure times ranging from ~ 200 s to ~ 3000 s. The cadence of the X-ray observations is variable, but data were taken at least once per day. We discarded the observation taken on 21 June 2018 at 11:47:14 UT, as the data were heavily affected by a hot column right at the SN 2018cow position.

All observations were reduced using the *Swift* software[3]. First, we reprocessed the data using the routine XRT-PIPELINE. Then, the routines XSELECT and XIMAGE were

[3] http://www.swift.ac.uk/analysis/xrt/setup.php
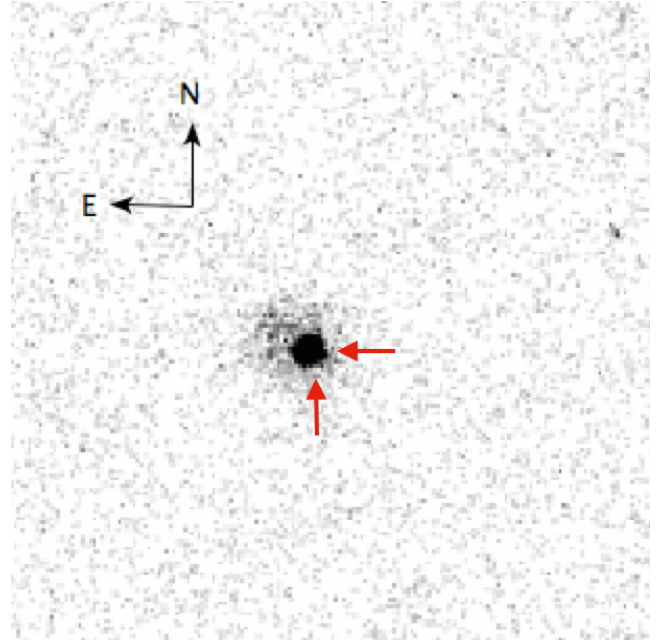
Figure 1. *Swift*/UVOT ultraviolet image of SN 2018cow taken during the X-ray luminosity increase on 29 June 2018 in the filter UVM2. The extended emission surrounding the object is likely due to its host galaxy. The image is 3′ × 3′. No increase in the UVM2 magnitude was observed during this episode. The arrows indicate the position of SN 2018cow.

used to measure count rates in the 0.3–10 keV energy band. We adopted a threshold signal-to-noise ratio of 3 for detections. To determine rate correction factors due to bad columns we used the routine XRTLCCORR.

For the spectral analysis we followed the SWIFT thread[4]. We used XRTMKARF to create the ancillary response files. For the spectral fitting we used the software package XSPEC (v12.9.1 Arnaud 1996). To model the hydrogen column density N$_H$ we used the model *tbnew_gas*[5] with WILM abundances (Wilms et al. 2000) and VERN cross-sections (Verner et al. 1996). We fitted our spectra with a power-law model (PEGPWRLW). For the spectrum presented in Figure 3 the data were grouped to have at least 15 counts per bin.

3   RESULTS

In Figure 2 we show the *Swift* 0.3-10 keV light curve of SN 2018cow from 19 June 2018 UT to 13 July 2018 UT. Data behind this Figure are reported in Table A1. We see that SN 2018cow shows a variable behavior on time scales of days. There are multiple re-brightenings after the first detection on 19 June 2018 UT. The most significant increase in the X-ray count rate is the one detected on 29 June 2018 (09:21:01 UT[6]), with a rate of 0.35 ± 0.05 counts s^{-1} (see also Figure 1). Fitting an absorbed power-law model to that observation,

[4] http://www.swift.ac.uk/analysis/xrt/spectra.php
[5] http://pulsar.sternwarte.uni-erlangen.de/wilms/research/tbabs/
[6] This observation was not affected by a hot column, unlike the longer observation recorded at 09:24:14 UT.
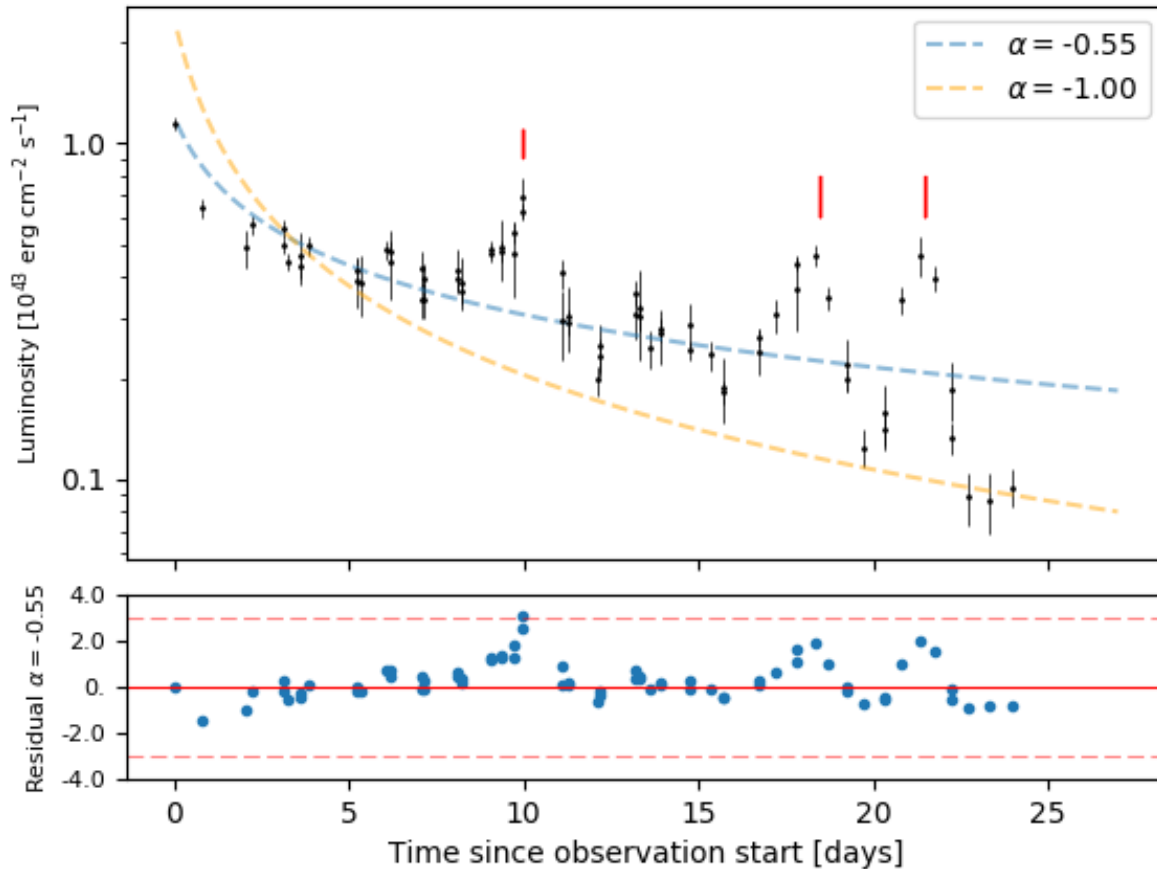
Figure 2. X-ray *Swift* light curve of SN 2018cow from 19 June 2018 (10:34:53 UT) to 13 July 2018 (09:56:36 UT) in the 0.3-10 keV energy band. A power-law fit with $\alpha = -0.55 \pm 0.01$ (where $L_X \propto t^{\alpha}$) is shown (blue line). Significant deviations appear during the episodes in which the X-ray luminosity increased. For comparison, we also plotted a fit with $\alpha = -1$ (orange line). Residuals normalized to the rms error are shown in the bottom part of the plot. The dashed lines indicate the 3σ level. The presence of consecutive excesses, increases the detection significance of the events (indicated by the red vertical lines). A table with the data is given in the Appendix.

Rivera Sandoval & Maccarone (2018c) determined an X-ray flux in the 0.3-10 keV of $(1.8 \pm 0.7) \times 10^{-11}$ erg cm^{-2} s^{-1} and $\Gamma = 1.2 \pm 0.8$ which represented a flux increase of approximately a factor of two with respect to the observations taken on 21 June 2018 (16:37:11 UT), when the object had a flux of $(1.2 \pm 0.2) \times 10^{-11}$ erg cm^{-2} s^{-1} and $\Gamma = 1.8 \pm 0.3$ (Sandoval et al. 2018).
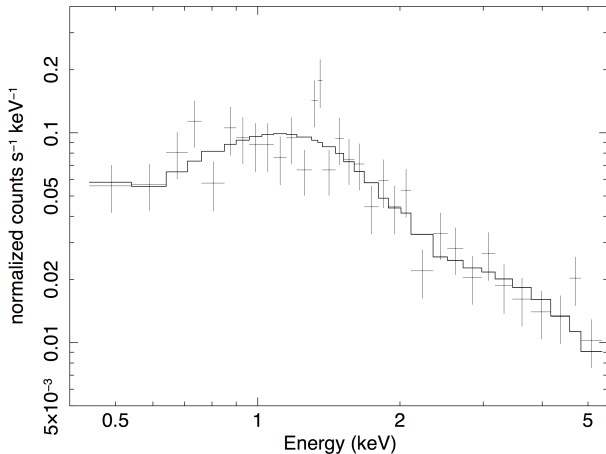
The X-ray spectrum of SN 2018cow in the 0.3-10 keV band can be described by a power-law model with $\Gamma \lesssim 2$ (Figure 3) at all epochs. There is no evidence for spectral evolution in the 0.3-10 keV band since discovery, and no evidence for significant spectral evolution during the X-ray increases (measurements are consistent within 90% errors). The value of the spectral index is in agreement with observations carried out with *Chandra* and *NICER* (Maccarone et al. 2018; Miller et al. 2018) and also with *NuSTAR* and *INTEGRAL* at higher energies (Margutti et al. 2018; Grefenstette et al. 2018; Savchenko et al. 2018). Though, indications of a hard component at energies above 15 keV was

found on 23 June 2018 (Margutti et al. 2018), which was not longer observed on 2 July 2018 (Grefenstette et al. 2018). The combined spectrum of SN 2018cow up to 13 July 2018 can be described with a $\Gamma \sim 1.6$.

Assuming a decay of the luminosity $L_X \propto t^{\alpha}$, we found that the temporal evolution of the 0.3–10 keV luminosity can be best fitted with a power-law index $\alpha = -0.55 \pm 0.01$ (figure 2), which is not consistent with the one found by *INTEGRAL*, where $\alpha = -1$ (Savchenko et al. 2018). The X-ray increases shown in the light curve of SN 2018cow seem to significantly deviate from that fit. The presence of consecutive excesses in the residuals, give us confidence on the significance of these events.

4 DISCUSSION

SN 2018cow has been classified as a candidate SN due to its optical spectral properties(Xu et al. 2018; Perley et al.

Figure 3. X-ray spectrum of SN 2018cow in the 0.3-10keV energy band, using a ~ 3 ks *Swift* observation taken on 7 July 2018. The spectrum can be described with a photon index $\Gamma = 1.4 \pm 0.2$. The X-ray flux was $(1.1 \pm 0.1) \times 10^{-11}$ erg cm^{-2} s^{-1}. Quoted errors are at 90% confidence level.

2018; Benetti et al. 2018). However, an unambiguous classification remains to be established. If indeed SN 2018cow is a SN, its variable X-ray behavior (Fig. 2) could be explained as due to the interaction of the SN shock with non-uniform circum-stellar material (CSM), perhaps related to eruptive, Luminous Blue Variable (LBV)-like mass-loss from the pre-supernova progenitor. Assuming a wind velocity $v_{wind} \sim 1000$ km s^{-1} (typical for Type Ib/Ic SN; Wellons et al. 2012), and a SN expansion velocity $v_{SN} \sim 20,000$ km s^{-1} as determined for SN 2018cow from optical spectroscopy (Izzo et al. 2018), then the ~ 10 days between the first two X-ray peaks (linked to interactions between the SN and the LBV-like ejecta) would correspond to LBV-like eruptions spaced by ~ 200 days. This value is consistent with pulsations of some LVB stars (Lamers et al. 1998). Note, however, that the mass-ejections from the progenitor could have been neither at a constant rate nor at a constant velocity. This would help explain the variable frequency of the observed increases in the X-ray light curve, such as the occurrence of the last one.

Flux increases in the X-ray light curves of Type Ib/Ic SNe are not commonly observed within few weeks after the explosion. Usually these light curves follow smooth decays (e.g. Modjaz et al. 2009; Campana et al. 2006a). However, there are records of X-ray flux variations in some SNe due to strong interaction with the CSM (e.g. Immler et al. 2008), which supports the idea that the variations observed in the X-ray light curve of SN 2018cow could be indeed caused by a similar mechanism, though with different factors affecting the timescale of occurrence of the re-brightening episodes. GRB X-ray afterglows also show increases in their light curve. However, they occur at time scales much shorter than those observed for the SN 2018cow (see e.g. Campana et al. 2006b; Ruffini et al. 2018).

In order to determine the nature of SN 2018cow X-ray emission, we estimated the radio-to-X-ray spectral index comparing the 34 GHz flux (~ 5.6 mJy; Dobie et al. 2018a) measured on 26 June 2018 (09:00-14:00 UT), to the *Swift* X-ray flux of two measurements taken the same

day within that time interval (13:06:00-13:21:53 UT, $F_X = 9.2 \times 10^{-12}$ erg cm^{-2} s^{-1}/2.4×10^{17} Hz $\approx 4 \times 10^{-6}$ mJy). We obtained $\Gamma_r \approx 1.9$. This value is in agreement with the X-ray spectral index obtained from the *Swift* data. It is also in agreement with results for other CSM-interacting BL-Ic SNe (Corsi et al. 2014) in which the X-rays seem to have a synchrotron origin. This suggests that a similar mechanism may be powering SN 2018cow X-ray emission.

Follow-up observations of SN 2018cow at all the wavelengths will likely allow to obtain more insights about its nature. However, whatever its classification, SN 2018cow is already an outstanding object due to the time variability of its X-ray light curve, and to its peculiar multi-wavelength behavior in general.

REFERENCES

Arnaud K. A., 1996, in Jacoby G. H., Barnes J., eds, Astronomical Society of the Pacific Conference Series Vol. 101, Astronomical Data Analysis Software and Systems V. p. 17
Benetti S., Pastorello A., Cappellaro E., Turatto M., Tomasella L., Fiore A., Reguitti A., Gromadzki M., 2018, The Astronomer's Telegram, 11836
Bright J., Horesh A., Fender R., Motta S., Sfaradi I., Titterington D., Perrott Y., Ho A., 2018, The Astronomer's Telegram, 11774
Campana S., et al., 2006a, Nature, 442, 1008
Campana S., et al., 2006b, A&A, 454, 113
Corsi A., et al., 2014, ApJ, 782, 42
D'Avanzo P., et al., 2012, MNRAS, 425, 506
Dal Canton T., et al., 2018, The Astronomer's Telegram, 11793
Dobie D., Ravi V., Ho A., Kasliwal M., Murphy T., 2018a, The Astronomer's Telegram, 11795
Dobie D., Ravi V., Ho A., Kasliwal M., Murphy T., 2018b, The Astronomer's Telegram, 11818
Drout M. R., et al., 2016, ApJ, 821, 57
Garcia-Gonzalez J. A., Gonzalez M., Martinez I., HAWC Collaboration 2018, The Astronomer's Telegram, 11792
Grefenstette B., Margutti R., Chornock R., Metzger B., Migliori G., 2018, The Astronomer's Telegram, 11813
Immler S., et al., 2008, ApJ, 674, L85
Izzo L., et al., 2018, The Astronomer's Telegram, 11753
Jones D. O., Rojas-Bravo C., Dimitriadis G., Pan Y.-C., Foley R. J., 2018, The Astronomer's Telegram, 11736
Lamers H. J. G. L. M., Bastiaanse M. V., Aerts C., Spoon H. W. W., 1998, A&A, 335, 605
Lien A. Y., et al., 2018, The Astronomer's Telegram, 11782
Maccarone T. J., Sandoval L. R., Corsi A., Pooley D., Knigge C., 2018, The Astronomer's Telegram, 11779
Margutti R., Chornock R., Laskar T., Fong W., Grefenstette B., Risaliti G., 2018, The Astronomer's Telegram, 11775
Miller J. M., et al., 2018, The Astronomer's Telegram, 11773
Modjaz M., et al., 2009, ApJ, 702, 226
Perley D., 2018, The Astronomer's Telegram, 11732

Perley D. A., Blagorodnova N., Neill J. D., Walters R., 2018, The Astronomer's Telegram, 11776

Ramsay G., et al., 2001, A&A, 365, L294

Rivera Sandoval L. E., Maccarone T., 2018a, The Astronomer's Telegram, 11737

Rivera Sandoval L. E., Maccarone T., 2018b, The Astronomer's Telegram, 11739

Rivera Sandoval L. E., Maccarone T., 2018c, The Astronomer's Telegram, 11801

Ruffini R., et al., 2018, ApJ, 852, 53

Saitou K., Tsujimoto M., Ebisawa K., Ishida M., 2012, PASJ, 64, 88

Sandoval L. E. R., Maccarone T., Brown P., 2018, The Astronomer's Telegram, 11761

Savchenko V., Ferrigno C., Kuulkers E., Goetz D., Bozzo E. e. a., 2018, The Astronomer's Telegram, 11843

Smartt S. J., et al., 2018, The Astronomer's Telegram, 11727

Srivastav S., Singh A., Kumar B., Kumar H., Bhalerao V., Anupama G. C., Sahu D. K., Bandyopadhyay A., 2018, The Astronomer's Telegram, 11766

Verner D. A., Ferland G. J., Korista K. T., Yakovlev D. G., 1996, ApJ, 465, 487

Warner B., 1987, MNRAS, 227, 23

Wellons S., Soderberg A. M., Chevalier R. A., 2012, ApJ, 752, 17

Wilms J., Allen A., McCray R., 2000, ApJ, 542, 914

Xu D., et al., 2018, The Astronomer's Telegram, 11740

de Ugarte Postigo A., et al., 2018, The Astronomer's Telegram, 11749

APPENDIX A: SWIFT X-RAY LIGHT CURVE DATA

We present the *Swift* data used to generate figure 2 in Section 3.

This paper has been typeset from a TeX/LaTeX file prepared by the author.

Table A1. *Swift* X-ray light curve of SN 2018cow in the 0.3–10keV. The time since the first observation (19 June 2018 at 10:34:53 UT) is indicated in column 1. We have used a factor of 1.97×10^{43} erg cm^{-2} s^{-1} to convert the count rates to luminosities.

t (days)	Luminosity (10^{43} erg cm^{-2} s^{-1})	σ_{L_X} (10^{43} erg cm^{-2} s^{-1})
0.000	1.147	0.051
0.781	0.642	0.041
2.047	0.488	0.061
2.252	0.573	0.036
3.116	0.557	0.038
3.116	0.496	0.028
3.251	0.444	0.028
3.639	0.460	0.081
3.641	0.431	0.034
3.838	0.496	0.030
5.233	0.391	0.065
5.236	0.419	0.038
5.366	0.383	0.077
6.099	0.484	0.032
6.165	0.446	0.103
6.168	0.474	0.036
7.105	0.425	0.053
7.110	0.344	0.041
7.167	0.393	0.043
7.170	0.342	0.041
8.096	0.421	0.065
8.099	0.393	0.030
8.231	0.387	0.067
8.234	0.363	0.030
9.091	0.472	0.028
9.093	0.486	0.030
9.356	0.492	0.101
9.358	0.480	0.036
9.752	0.468	0.118
9.754	0.543	0.038
9.949	0.697	0.095
9.951	0.628	0.038

Table A1. Continued

t (days)	Luminosity (10^{43} erg cm^{-2} s^{-1})	σ_{L_X} (10^{43} erg cm^{-2} s^{-1})
11.078	0.296	0.069
11.080	0.411	0.041
11.277	0.306	0.067
11.279	0.294	0.026
12.143	0.197	0.020
12.207	0.249	0.041
12.209	0.231	0.030
13.205	0.310	0.049
13.209	0.359	0.032
13.346	0.324	0.097
13.348	0.304	0.030
13.601	0.245	0.032
13.941	0.271	0.049
13.945	0.278	0.022
14.731	0.290	0.043
14.734	0.243	0.016
15.339	0.235	0.024
15.728	0.188	0.041
15.730	0.182	0.014
16.724	0.241	0.038
16.727	0.265	0.018
17.194	0.308	0.036
17.788	0.369	0.093
17.789	0.438	0.020
18.329	0.464	0.034
18.719	0.348	0.028
19.253	0.221	0.039
19.255	0.197	0.016
19.714	0.124	0.016
20.320	0.158	0.032
20.322	0.140	0.018
20.783	0.342	0.030
21.333	0.462	0.063
21.773	0.397	0.032
22.242	0.186	0.038
22.244	0.132	0.014
22.715	0.089	0.016
23.315	0.087	0.018
23.973	0.095	0.012